



Poly(7-oxanorbornenes) carrying 2,2,6,6-tetramethylpiperidine-1-oxy (TEMPO) radicals: Synthesis and charge/discharge properties

Jinqing Qu^a, Toru Katsumata^b, Masaharu Satoh^c, Jun Wada^d, Toshio Masuda^{b,*}

^a School of Chemistry and Chemical Engineering, South China University of Technology, Guangzhou, Guangdong 510640, China

^b Department of Polymer Chemistry, Graduate School of Engineering, Kyoto University, Katsura Campus, Kyoto 615-8510, Japan

^c Murata Manufacturing Co., Ltd., 1-10-1 Higashikotari, Nagaokakyo-shi, Kyoto 520-2393, Japan

^d Corporate Planning Department, Nippon Kasei Chemical Co., Ltd., 1-8-8 Shinkawa, Chuoku, Tokyo 104-0033, Japan

ARTICLE INFO

Article history:

Received 12 October 2008

Received in revised form

15 November 2008

Accepted 18 November 2008

Available online 28 November 2008

Keywords:

Charge–discharge properties

Electro-chemistry

Organic radical battery

ABSTRACT

TEMPO-containing 7-oxanorbornene monomers **1–4** (TEMPO = 2,2,6,6-tetramethylpiperidine-1-oxy) were synthesized and polymerized via ring-opening metathesis using a ruthenium carbene catalyst. Monomers **1** and **3** gave polymers with number-average weights of 80 100 and 112 200 in 85 and 96% yields, respectively, whereas monomers **2** and **4** did not provide high molecular weight polymers. Poly(**1**) and poly(**3**) were soluble in common solvents including CHCl₃, CH₂Cl₂ and THF, while insoluble in hexane, diethyl ether and MeOH. They were thermally stable up to ca. 240 °C according to the TGA measurements in air. The secondary batteries utilizing the present polymers as cathode-active material demonstrated reversible charge/discharge processes, whose discharge capacities were 107 and 92.8 Ah/kg, and displayed excellent high-rate charge and discharge properties. These cells demonstrated excellent cycle life, e.g., the discharge capacities of poly(**1**) and poly(**3**) showed less than 10% decrements even after 100 cycles.

© 2008 Elsevier Ltd. All rights reserved.

1. Introduction

2,2,6,6-Tetramethyl-1-piperidine-1-oxy (TEMPO) and its derivatives are well-known stable nitroxyl radicals and have found applications in a variety of fields such as spin labels in the study of conformation and structural mobility of biological systems [1], scavengers of unstable radical species [2], and oxidizing agents [3]. The TEMPO radical is a typical oxygen-centered radical involving a resonance structure in which the odd electron is more or less delocalized to nitrogen, which contributes to its high stability. The TEMPO radical displays two redox couples, namely, oxidation to a cation and reduction to an anion. It can be oxidized to form the corresponding oxoammonium cation; the oxidation process of the radical is reversible and leads to p-type doping of the radical material. It can also be reduced to the aminoxy anion resulting in n-type doping of the material. By using the oxidation process to the cation, TEMPO-carrying polymers can be applied to cathode-active materials in secondary batteries, and such batteries can be called organic radical batteries (ORBs). ORBs offer numerous advantages

over lithium-ion batteries; in particular, the absence of heavy metals makes ORBs more environmentally friendly and safe, in which the positive electrode material (e.g., LiCoO₂) used in lithium-ion batteries are replaced by suitable nitroxide polymers in ORBs. ORBs can be charged and discharged quickly, and display a large number of battery charge/discharge cycles in addition to high charge and energy density [4,5].

We have reported the synthesis and charge/discharge properties of a few TEMPO-containing polyacetylenes and polynorbornenes that serve as charge-storage materials in ORBs, among which the discharge capacity of poly(NB-2,3-endo,exo-(COO-4-TEMPO)₂) (NB = norbornene) practically reaches its theoretical value (109 Ah/kg) [6]. Polyacetylenes and polynorbornenes containing the PROXY (PROXY = 2,2,5,5-tetramethylpyrrolidine-1-oxy) moieties have also been investigated, and some of these polymers displayed high capacity (up to 117 Ah/kg) and quick discharge properties [7]. More recently, we have reported TEMPO-containing cellulose derivatives [8] and DNA–cationic lipid complexes [9] as the positive electrode material of ORB and found that they displayed two-stage discharge process. The total capacity of one TEMPO-containing DNA–cationic lipid complex reached 192% of the theoretical value for one electron redox reaction, suggesting two-electron redox reactions between the cation and the anion.

Allcock et al. [10] have indicated that poly(7-oxanorbornenes) exist in a variety of microstructures, that it can interact with metal

* Corresponding author. Present address: Department of Environmental and Biotechnological Frontier Engineer, Fukui University of Technology, 3-6-1 Gakuen, Fukui 910-8505, Japan. Tel.: +81 75 383 2589; fax: +81 75 383 2590.

E-mail address: masuda@adv.polym.kyoto-u.ac.jp (T. Masuda).

cations via oxygen in the polymer backbone, and that the introduction of the oxygen atoms into the backbone of polynorbornenes raises the glass transition temperature which often lowers ionic conductivity, but the skeletal oxygen atoms also facilitate lithium-ion transport. Thus, it seems of interest to determine whether the poly(7-oxanorbornene) skeleton provides an advantage over the polynorbornene backbone in polymers with pendent TEMPO side chains. Here we synthesized various TEMPO-carrying polynorbornenes by direct polymerization of the corresponding monomers (Scheme 1) with a ruthenium-based metathesis catalyst, and clarified their fundamental properties and charge/discharge characteristics of the formed polymers as cathode-active materials in ORBs.

2. Experimental

2.1. Materials

The solvents used for polymerization were distilled according to the standard procedures before use. The Grubbs 2nd-generation catalyst was offered from Materia, Inc., and used as-received. 4-Amino-TEMPO (TCI), 4-hydroxy-TEMPO (TCI), *exo*-3,6-epoxy-1,2,3,6-tetrahydrophthalic anhydride (Aldrich), *N*-(3-dimethylaminopropyl)-*N'*-ethylcarbodiimide hydrochloride (EDC·HCl; Eiwiss Chemical Corporation), and 4-dimethylaminopyridine (DMAP; Wako) were purchased and used without further purification.

2.2. Measurements

^1H (400 MHz) and ^{13}C (100 MHz) NMR spectra were recorded on a JEOL EX-400 spectrometer using tetramethylsilane as an internal standard. IR spectra were measured on JASCO FT/IR-4100 spectrophotometers. Melting points (mp) were determined with a Yanaco micro melting point apparatus and elemental analyses were conducted at the Kyoto University Elemental Analysis Center. The number- and weight-average molecular weights (M_n and M_w) of polymers were determined by gel permeation chromatography (GPC) on a JASCO Gulliver system (PU-980, CO-965, RI-930, and UV-1570) equipped with polystyrene gel columns (Shodex columns KF-805L \times 3), using tetrahydrofuran (THF) as an eluent at a flow rate of 1.0 mL/min, calibrated with polystyrene standards at 40 °C. Cyclic voltammograms were observed with an HCH Instruments ALS600A-n electrochemical analyzer. The measurements were carried out with a modified ITO substrate as the working electrode coupled with a Pt plate counter electrode and an Ag/AgCl reference electrode, using a solution of a polymer (1 mM) and tetrabutylammonium perchlorate (TBAP, 0.1 M) in CH_2Cl_2 . Thermal gravimetric analysis (TGA) was carried out on a Perkin-Elmer TGA-7.

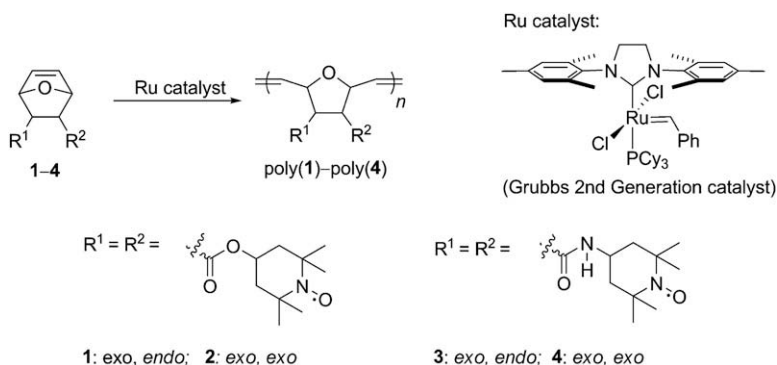
2.3. Monomer synthesis

Monomer **1** was synthesized as follows: *exo*-3,6-epoxy-1,2,3,6-tetrahydrophthalic anhydride (0.66 g, 4.00 mmol) was added to a solution of EDC·HCl (3.03 g, 8.80 mmol) and DMAP (1.08 g, 8.80 mmol) in CH_2Cl_2 (80 mL) at room temperature. 4-Hydroxy-TEMPO (1.52 g, 8.80 mmol) was added to the solution, and the resulting mixture was stirred at room temperature overnight. The reaction mixture was washed with water (100 mL) three times, and the organic layer was dried over anhydrous MgSO_4 . After filtration, the solvent was removed to afford a crude product, which was a mixture of monomers **1**, **2** (composition **1**:**2** = 2:1), and other compounds. Monomers **1** and **2** were isolated by flash column chromatography (eluent: ethyl acetate/hexane = 1/1). Yield 20%, pastel magenta red solid, mp 183.0–184.0 °C. IR (KBr, cm^{-1}): 3439, 2996, 2975, 2939, 1725, 1465, 1377, 1364, 1320, 1300, 1288, 1205, 1174, 1154, 1007, 986, 867, 724. Anal. Calcd for $\text{C}_{26}\text{H}_{40}\text{N}_2\text{O}_7$: C, 63.39; H, 8.18; N, 5.69. Found: C, 63.78; H, 8.30; N, 5.79.

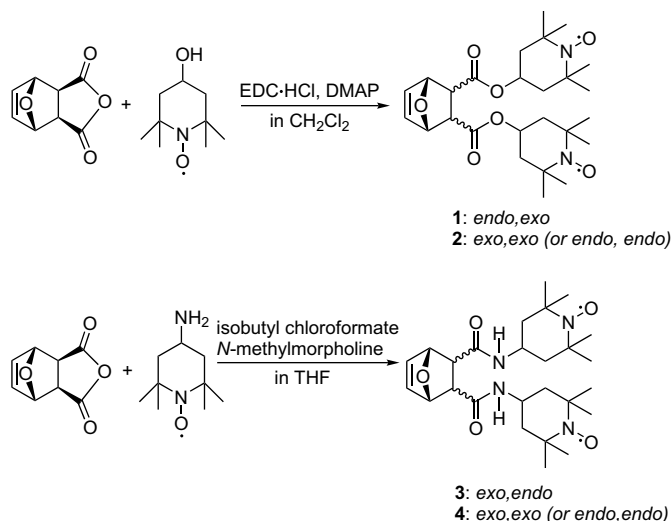
Monomer **2** was synthesized from *exo*-3,6-epoxy-1,2,3,6-tetrahydrophthalic anhydride and 4-hydroxy-TEMPO in the same way as **1**, and separated from monomer **1** by flash column chromatography. Yield 16%, pastel magenta red solid, mp 175.0–176.0 °C. IR (KBr, cm^{-1}): 3434, 2997, 2974, 2934, 1723 ($\nu_{\text{C=O}}$), 1465, 1364, 1318, 1301, 1240, 1003, 979, 774, 699, 642. Anal. Calcd for $\text{C}_{26}\text{H}_{40}\text{N}_2\text{O}_7$: C, 63.39; H, 8.18; N, 5.69. Found: C, 63.52; H, 8.42; N, 5.56.

Monomer **3** was prepared as follows: *N*-methylmorpholine (0.80 g, 8.0 mmol) was added to a solution of *exo*-3,6-epoxy-1,2,3,6-tetrahydrophthalic anhydride (0.66 mg, 4.0 mmol) in THF (15 mL) at room temperature. Isobutyl chloroformate (1.1 g, 8.0 mmol) was added to the solution to precipitate *N*-methylmorpholine hydrochloride as a white mass. Then, 4-amino-TEMPO (1.51 g, 8.5 mmol) was added, and the resulting mixture was stirred at room temperature overnight. The precipitate was removed by filtration, and the filtrate was concentrated by rotary evaporation. The residue was dissolved in ethyl acetate (50 mL) and washed with water three times, and dried over anhydrous MgSO_4 . After filtration, the solvent was removed to afford the crude product, which was a mixture of monomers **3**, **4** (composition **3**:**4** = 1.5:1), and other compounds. Monomer **3** was separated by flash column chromatography from hexane/ethyl acetate (1/1 volume ratio). Yield 14%, pastel magenta red solid, mp 126.0–127.0 °C. IR (KBr, cm^{-1}): 3542, 3365, 2970, 2872, 1727, 1672, 1539, 1465, 1394, 1377, 1365, 1241, 1184, 1052, 992, 973, 867, 673, 566. Anal. Calcd for $\text{C}_{26}\text{H}_{42}\text{N}_4\text{O}_5$: C, 63.65; H, 8.63; N, 11.42. Found: C, 63.78; H, 8.90; N, 11.75.

Monomer **4** was synthesized from *exo*-3,6-epoxy-1,2,3,6-tetrahydrophthalic anhydride and 4-amino-TEMPO in the same way as **3**, and separated from monomer **3** by flash column chromatography. Yield 9.0%, pastel magenta red solid, mp 117.0–118.0 °C. IR



Scheme 1. Polymerization of monomers 1–4.



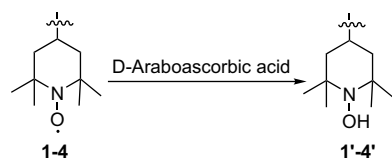
Scheme 2. Synthesis of monomers **1–4**.

(KBr, cm^{-1}): 3542, 3289, 2974, 2938, 2873, 1712, 1654, 1536, 1458, 1393, 1376, 1364, 1236, 1179, 1031, 981, 958, 869, 669, 566. Anal. Calcd for $\text{C}_{26}\text{H}_{42}\text{N}_4\text{O}_5$: C, 63.65; H, 8.63; N, 11.42. Found: C, 63.48; H, 8.70; N, 11.65.

Since it was impossible to measure the NMR spectra of monomers, the ^1H and ^{13}C NMR spectra of hydroxyamine compounds (**1'–4'**; Scheme 3) were examined, whose data are as follows. **1'**: ^1H NMR (400 MHz, CDCl_3 , δ): 5.79 [1H, =CH–CH–CH–COO(*endo*)], 5.59 [1H, =CH–CH–CH–COO(*exo*)], 5.26 [1H, –COO(*endo*)–CH<], 5.19 [1H, –COO(*exo*)–CH<], 5.10 [1H, =CH–CH–CH–COO(*endo*)], 5.08 [1H, =CH–CH–CH–COO(*exo*)], 3.32 [1H, –O–CHCH–COO(*endo*)], 3.24 [1H, –O–CHCH–COO(*exo*)], 1.78–1.42 (8H, –OCH CH_2C –), 1.20 (24H, >C(CH_3) $_2$). ^{13}C NMR (100 MHz, CDCl_3 , δ): 173.1 (C=O), 172.5 (C=O), 136.3, 135.7, 81.9, 79.7, 63.9, 64.1, 45.4, 43.5, 42.5, 41.7, 41.6, 40.5, 20.9. **2'**: ^1H NMR (400 MHz, CDCl_3 , δ): 5.69 (2H, =CH–), 5.24 (2H, –COO–CH<), 5.08 (2H, =CH–CH–O), 3.28 (2H, –O–CHCH–COO–), 1.68–1.40 (8H, –OCH CH_2C –), 1.16 (24H, >C(CH_3) $_2$). ^{13}C NMR (100 MHz, CDCl_3 , δ): 171.8, 134.8, 81.6, 63.5, 45.2, 42.7, 41.3, 19.0. **3'**: ^1H NMR (400 MHz, CDCl_3 , δ): 6.01 [1H, =CH=CH–CH–CONH(*endo*)], 5.91 [1H, =CH–CH–CH–CONH(*exo*)], 4.69 [1H, =CH–CH–CH–CONH(*endo*)], 4.58 [1H, =CH–CH–CH–CONH(*exo*)], 3.54 [1H, >CHNHCO(*endo*)], 3.48 [1H, >CHNHCO(*exo*)], 3.12 [1H, –O–CHCH–CONH(*endo*)], 3.04 [1H, –O–CHCH–CONH(*exo*)], 1.78–1.40 (8H, –OCH CH_2C –), 1.17 (24H, >C(CH_3) $_2$). ^{13}C NMR (100 MHz, CDCl_3 , δ): 172.8 (C=O), 172.3 (C=O), 136.1, 135.8, 80.9, 80.6, 56.8, 57.1, 45.8, 45.1, 40.9, 40.5, 34.8, 34.2, 21.9. **4'**: ^1H NMR (400 MHz, CDCl_3 , δ): 5.89 (2H, =CH–), 4.84 (2H, =CHCHO), 3.50 (2H, NHCH<), 3.10 (2H, –O–CHCH–COO–), 1.80–1.50 (8H, –OCH CH_2C –), 1.16 (24H, >C(CH_3) $_2$). ^{13}C NMR (100 MHz, CDCl_3 , δ): 174.3, 135.6, 79.6, 57.9, 45.1, 41.0, 34.5, 20.9.

2.4. Polymerization procedures

Polymerizations (ROMP) of oxanorbornene monomers **1–4** were carried with the Grubbs 2nd-generation catalyst in dry CH_2Cl_2 at 30°C for 2 h under the following conditions: $[\text{monomer}]_0 = 0.50\text{ M}$,



Scheme 3. Synthesis of hydroxylamine compounds **1'–4'**.

[catalyst] = 5.0 mM. The polymerization was quenched by adding *tert*-butyl vinyl ether (0.20 mL) and stirring the mixture at room temperature for 1 h. The polymers were isolated by precipitation in diethyl ether.

2.5. Spectroscopic data of the polymers

IR (KBr, cm^{-1}) data of the polymers: poly(**1**): 3447, 2976, 2939, 1734, 1465, 1364, 1240, 1160, 1007, 986, 810, 683, 558. Poly(**3**): 3474, 2973, 2939, 1734, 1655, 1559, 1542, 1509, 1466, 1378, 1365, 1217, 1040, 996, 849, 754, 669, 560.

2.6. Fabrication and electrochemical measurements of batteries using polymers

A coin-type cell was fabricated by stacking electrodes (1.13 cm^2) with porous polyolefin separator films. A cathode was formed by pressing the composites of a polymer (10 wt%), carbon fiber (80 wt%), and fluorinated polyolefin binder (10 wt%) as described in a previous paper [6a]. The cathode was set to a coin-type cell possessing a lithium metal anode. A composite solution of ethylene carbonate (30 vol%)/diethyl carbonate (70 vol%) containing 1 M of LiPF_6 was used as an electrolyte. Charge/discharge properties were measured at 25°C using a computer controlled automatic battery charge and discharge instrument (Keisokukiki Co. Ltd., Battery Labo System BLS5500).

2.7. Theoretical capacity of polymer-based cell

The theoretical capacity (in A h/kg) of an electroactive polymer was calculated from the molecular weight required per exchangeable unit charge in a polymer [6b]:

$$C(\text{A h/kg}) = \frac{N_A \times e}{3600 \times (M_w/1000)}$$

where $N_A \times e$ is the Faraday constant (96 487 C/mol), while M_w is the equivalent weight (or mass) of polymer in g, and defined as the molecular weight (molar mass) of repeating unit of polymer divided by the number of electrons exchanged or stored by it (which may be a fractional number), or as the molecular weight of the set of repeating units exchanging (storing) one electron in polymers.

3. Results and discussion

3.1. Monomer synthesis

Oxanorbornene monomers **1–4** were synthesized by the condensation of an *exo*-anhydride derivative of 7-oxanorbornene with hydroxy or amino functionality of the TEMPO derivatives (Scheme 2). These reactions are similar to those of the 5-norbornene-*endo*-2,3-dicarboxylic anhydride condensation with 4-hydroxy-TEMPO [6a,d], and all these reactions provide a mixture of two isomers, namely, *exo/exo* (or *endo/endo*) and *endo/exo* diester or diamide derivatives. Thus, the products of the present monomer syntheses contained two configurational isomers [*exo/exo* (or *endo/endo*) and *endo/exo*], and so these isomers were separated by flash column chromatography (eluent: ethyl acetate/hexane = 1/1).

Since it was impossible to measure the high-resolution ^1H and ^{13}C NMR spectra of the monomers due to the presence of free radicals, they were converted into the corresponding hydroxy compounds in order to measure their NMR spectra (Scheme 3). The hydroxy compounds **2'** and **4'** that were derived from **2** and **4** showed single peaks based on the carbonyl and olefinic carbons in the ^{13}C NMR spectrum, from which the *exo* orientation for both

Table 1
Polymerization of monomers **1–4** with the Grubbs 2nd-generation catalyst.

Run	Monomer	Polymer ^c		
		Yield, %	M_n^d	M_w/M_n^d
1 ^a	1	85	80 100	2.24
2 ^a	2	86	1190	2.74
3 ^b	3	96	112 200	2.78
4 ^b	4	Trace	—	—

^a In CH₂Cl₂, 45 min, 30 °C; [M]₀ = 0.50 M, [Ru] = 5.0 mM.

^b In CH₂Cl₂, 30 min, 30 °C; [M]₀ = 1.0 M, [Ru] = 10 mM.

^c MeOH-insoluble part.

^d Determined by GPC (THF, polystyrene calibration).

ester (or amide) groups can reasonably be concluded. On the other hand, **1'** and **3'** corresponding to **1** and **3** exhibited two carbonyl carbon signals and two olefinic carbon signals in the ¹³C NMR spectrum, thus providing the evidence that one of the ester groups is oriented in endo and the other in exo configuration. The structures of the monomers **1–4** were further confirmed by IR spectra and elemental analysis.

3.2. Polymerization

Table 1 summarizes the conditions and results of ROMP of monomers **1–4** using the Grubbs 2nd-generation catalyst. The polymerization mixtures of **1** and **3** became deep yellow within 30 min, and gradually turned dark brown with the concomitant increase of viscosity. After polymerization, the reaction mixture was poured into a large amount of methanol to precipitate the formed polymers. Monomers **1** and **3** gave polymers with high number-average molecular weights of 80,100 and 112,200 in 85 and 96% yields, respectively. On the other hand, the polymerization of **2** and **4** did not provide high molecular weight polymers even though the monomer concentration was increased to 2.0 M. These results suggest that monomers **2** and **4** are not exo, exo isomers but endo, endo isomers, because endo, endo isomers of norbornene and 7-oxanorbornene derivatives usually show low polymerizability

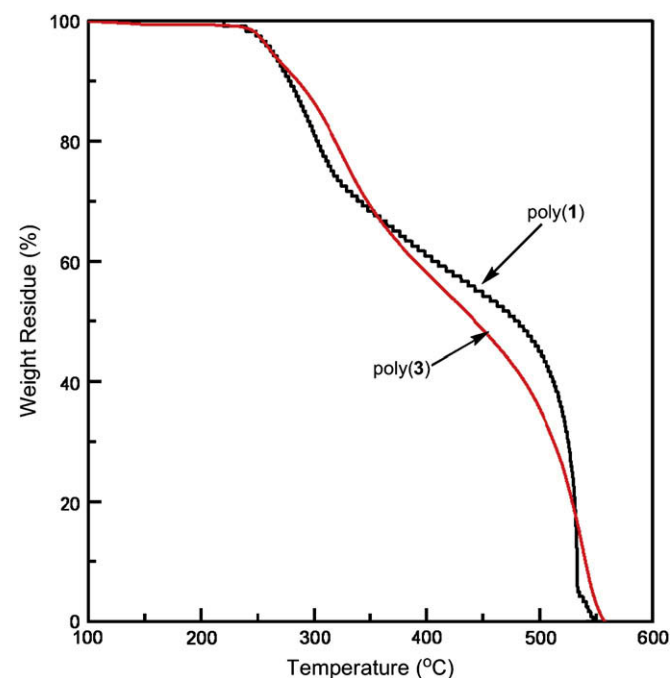


Fig. 1. TGA curves of poly(**1**) and poly(**3**).

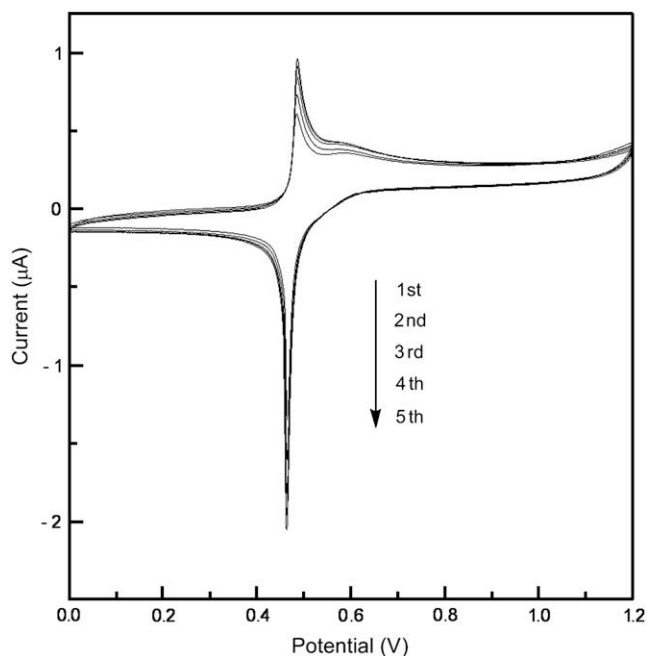


Fig. 2. Cyclic voltammograms of poly(**1**) and poly(**3**) measured at a scan rate of 0.01 V/s vs. Ag/Ag⁺ in TBAP solution.

compared to other isomers [11]. The NMR data of **1'–4'** also seem to support this speculation.

3.3. Characterization of the polymers

Though no evident information was obtained by IR and NMR spectroscopies, it is likely that poly(**1**) and poly(**3**) were formed by ROMP of the cycloolefin moiety. The IR spectra of these polymers showed a strong absorption peak at 1364 cm⁻¹ assignable to the stretching vibration of N–O• bond, indicating the incorporation of

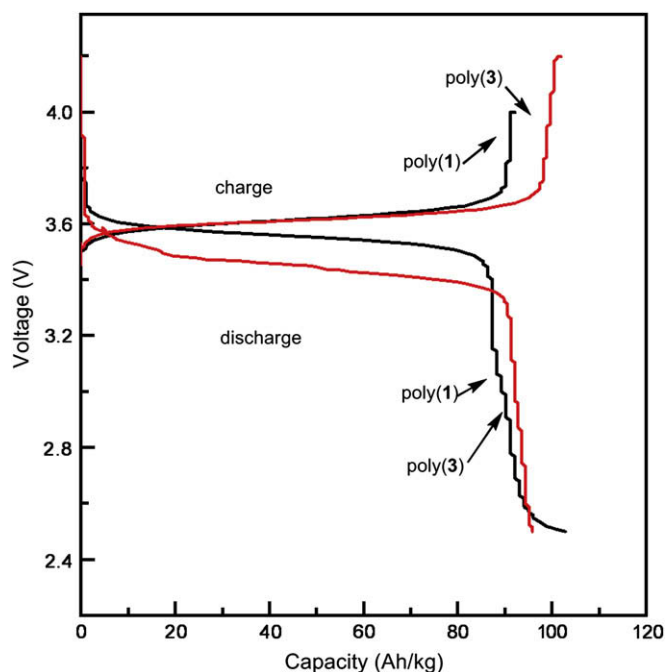
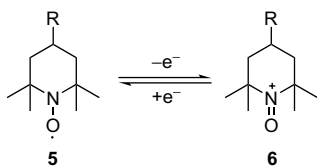


Fig. 3. Charge–discharge curves of poly(**1**) and poly(**3**) at a current density of 0.088 mA/cm² (0.09–0.115 A/g) in a range of 2.5–4.2 V cell voltage.



Scheme 4. The redox reactions of the TEMPO radical.

TEMPO moiety into the polymers. Poly(**1**) and poly(**3**) were soluble in relatively non-polar organic solvents including toluene, CHCl_3 , CH_2Cl_2 and THF, while insoluble in hexane, diethyl ether and methanol. Fig. 1 illustrates the TGA thermograms of poly(**1**) and poly(**3**), whose onset temperatures of weight loss were both about 240°C (under air) implying moderate thermal stability. The decomposition of the present polymers showed similar profiles, which suggests that the ester and amide linkages are cleaved at first followed by the degradation of the main chain.

Fig. 2 shows the cyclic voltammetry (CV) curves of poly(**1**), which displays reversible oxidation and reduction based on the TEMPO radical. Poly(**1**) exhibits an oxidation potential peak at 0.49 V vs. Ag/Ag^+ , and a reduction potential peak at 0.46 V vs. Ag/Ag^+ at a sweep rate of 0.01 V/s . Meanwhile poly(**3**) showed the corresponding peaks at 0.51 and 0.47 V , respectively (the CV curves of poly(**3**) are not shown). It is noted that the distances between the oxidation and reduction potential peaks of poly(**1**) and poly(**3**) are 0.03 and 0.04 V , respectively, which are by far smaller than those of other electroactive organic materials such as poly(2,2,6,6-tetramethylpiperidinyloxy methacrylate) (PTMA) (ca. 0.146 V) [4h]. The small gaps between the reduction and oxidation peaks generally imply large electrode reaction rates of the polymers, which suggest that these polymers will exert high power rates in the charge/discharge processes of battery under constant battery process conditions. The oxidation and reduction peaks of poly(**1**) and poly(**3**) scarcely changed after five CV scans, indicating that they are electrochemically quite stable.

3.4. Charge/discharge properties

The charge/discharge curves of the cells fabricated with poly(**1**) and poly(**3**) were measured at a constant current density of $0.088\text{ mA}/\text{cm}^2$ ($0.09\text{--}0.115\text{ A/g}$), in a cell voltage range of $2.5\text{--}4.2\text{ V}$. Fig. 3 shows clear voltage plateaus in both charge and discharge curves with both cells, advocating the applicability of the present polymers as cathode-active materials for a rechargeable battery. The plateau voltages of the charge/discharge processes were in a range of $3.4\text{--}3.8\text{ V}$ starting from approximately 3.6 V vs. Li/Li^+ , which corresponds to the redox potential of the TEMPO radical. It is reasonable to assume that the charge process at the cathode is oxidation of TEMPO moieties (**5**) in the polymers to oxoammonium salts (**6**), and the discharge process is the reverse reaction, namely, reduction of the salt (Scheme 4). Taking into account the fact that each TEMPO moiety releases one electron in this oxidation process, the theoretical capacities of the cells fabricated with poly(**1**) and

Table 2
Capacity data of polymers.

Polymer	m/e^a	Theoretical capacity, ^b A h/kg	Observed capacity, ^c A h/kg	Observed capacity/theoretical capacity, %
Poly(1)	246.3	108.9	107.0	98.3
Poly(3)	245.3	109.3	92.8	85.0

^a The polymer mass required per exchangeable unit.

^b Theoretical capacity (A h/kg), namely specific charge (in A h/kg) calculated according to references [6a,b].

^c Observed capacity (A h/kg): Initial discharge capacity at a current density of $0.088\text{ mA}/\text{cm}^2$ ($0.09\text{--}0.115\text{ A/g}$) and cut-off at 3.0 V .

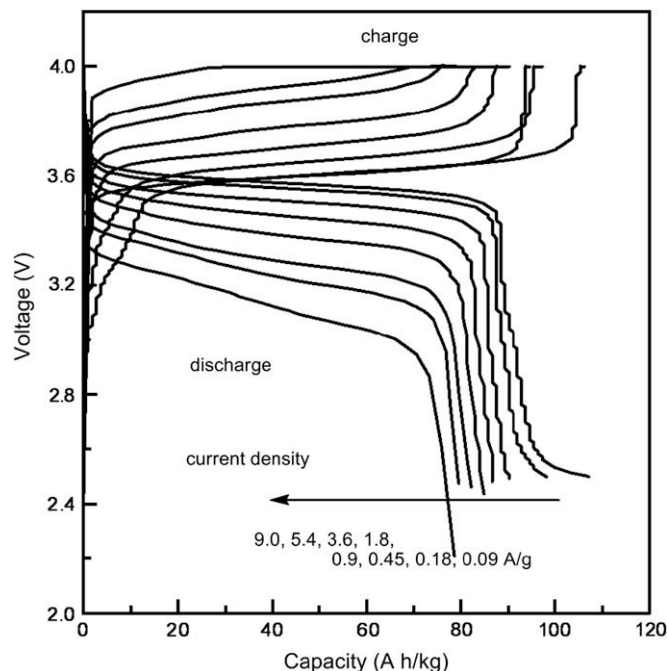


Fig. 4. Charge/discharge curves of poly(**1**) at different current rates in a range of $2.5\text{--}4.2\text{ V}$ cell voltage.

poly(**3**) were estimated to be 108.9 and 109.3 A h/kg , respectively (Table 2). The discharge capacities of the cells evaluated from the values at 2.5 V in Fig. 3 were observed as 107.0 and 92.8 A h/kg at a current density of $0.088\text{ mA}/\text{cm}^2$ ($0.09\text{--}0.115\text{ A/g}$). Interestingly, these values are pretty close to their theoretical ones.

Fig. 4 depicts the charge/discharge curves of poly(**1**) observed at different current densities. The charge and discharge capacities gradually decrease with increasing current densities, which is attributable to the polarization of TEMPO. An effective capacity of

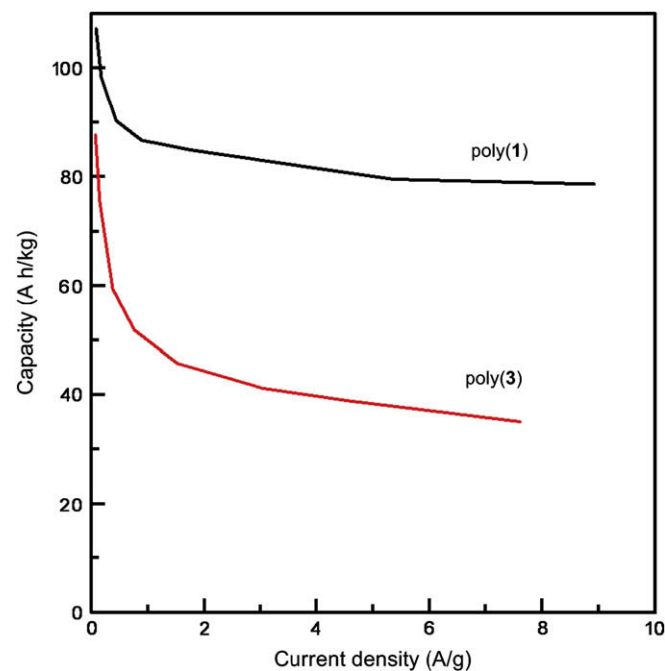


Fig. 5. Dependence of capacity on discharge rate curve of poly(**1**) and poly(**3**). Charge and discharge were repeated at a current density of $0.088\text{ mA}/\text{cm}^2$ ($0.09\text{--}0.115\text{ A/g}$) in a range of $3.0\text{--}4.0\text{ V}$ cell voltage.

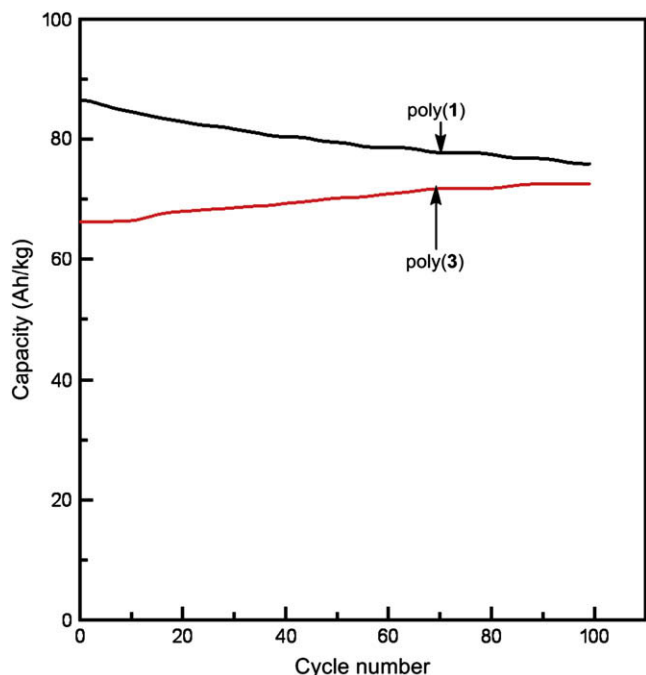


Fig. 6. Dependence of capacity on cycle number of poly(1) and poly(3). Charge and discharge were repeated at a current density of 0.088 mA/cm^2 ($0.09\text{--}0.115 \text{ A/g}$) in a range of $3.0\text{--}4.0 \text{ V}$ cell voltage.

ca. 78.0 A h/kg was attained at a current density of 9.0 A/g based on a cut-off voltage of 2.5 V with poly(1), which corresponds to 73% of the discharge capacity at 0.09 A/g , indicating that the poly(1)-based cell displays excellent charge/discharge characteristics under extremely large current. In Fig. 5, the discharge capacity at a current of 0.9 A/g was 83 A h/kg . This means that 76.2% of the theoretical capacity is available upon charge and discharge within 5.5 min [$= (83 \text{ A h/kg} \times 60 \text{ min/h}) / (0.9 \text{ A/g} \times 1000 \text{ g/kg})$]. According to this result, the power density is estimated as 2.66 kW/kg ($= 0.9 \text{ kA/kg} \times 2.96 \text{ V}$), when an average discharge voltage of 2.96 V is employed. It is noteworthy that this power density is much larger than that (ca. $0.6\text{--}1.0 \text{ kW/kg}$) of Li-ion batteries. These results demonstrate that poly(1) features fast charge and discharge.

Fig. 5 depicts the relationship between capacity and current densities of poly(1) and poly(3). The large capacity of poly(1) was maintained fairly well even though the current densities was increased to 9.0 A/g . On the other hand, the capacity of poly(3) decreased more sharply with increasing current densities. Thus large capacity is available in the discharge of especially poly(1) even at large current densities.

Fig. 6 illustrates the cycle performance of the poly(1) and poly(3)/Li cells, in which charge and discharge were repeated at 0.088 mA/cm^2 . The capacity of the cell using poly(1) maintained over 90% after 100 cycles. Poly(3) exhibited a different cycle performance; namely, the increase in capacity was observed, which appears to arise from the increase in the contact surface between the electrode and the electrolyte probably because of swelling of the polymer during the charge/discharge process. It seems that the cycle lives of poly(1) and poly(3)-based cells are comparable to those of the reported PTMA system [4].

4. Conclusions

In the present research, we have synthesized a group of 7-oxanorborene monomers containing TEMPO, **1–4**, and

polymerized them with a Ru catalyst. Monomers **1** and **3** provided polymers with number-average molecular weights of $80\,000\text{--}112\,000$ in $85\text{--}96\%$ yields. The capacity of the poly(1)- and poly(3)-based cells reached 107 and 92.8 A h/kg , respectively, corresponding to 98.3 and 85% of their theoretical capacity value. The cells fabricated with poly(1) and poly(3) as cathodes demonstrated a promising cycle life; i.e., their capacity hardly deteriorated even after 100 cycles. Charge-storage materials based on poly(1) and poly(3) can be applied to cathode-active materials in organic radical batteries, which feature quick charge/discharge and high power density.

Acknowledgements

The present research was partly supported by a Grant-in-Aid for Exploratory Research from JSPS. Thanks are also due to the Iketani Science and Technology Foundation for financial support. We acknowledge the offer of the Grubbs 2nd-generation catalyst by Materia, Inc. Jinqing Qu acknowledges the financial support from the Ministry of Education, Culture, Sports, Science, and Technology (Monbukagakusho), Japan.

References

- [1] (a) Martinez CG, Jockusch S, Ruzzi M, Sartori E, Moscatelli A, Turro NJ, et al. *J Phys Chem A* 2005;109:10216–21; (b) Matsuda K, Stone MT, Moore JS. *J Am Chem Soc* 2002;124:11836–7.
- [2] (a) Hawker CJ, Bosman AW, Harth E. *Chem Rev* 2001;101:3661–88; (b) Beckwith ALJ, Bowry VW, Ingold KU. *J Am Chem Soc* 1992;114:4983–92.
- [3] (a) Anderson CD, Shea KJ, Rychnovsky SD. *Org Lett* 2005;7:4879–82; (b) Ferreira P, Phillips E, Rippon D, Tsang SC, Hayes W. *J Org Chem* 2004;69:6851–9; (c) Tanyeli C, Gümüş A. *Tetrahedron Lett* 2003;44:1639–42; (d) MacCorquodale F, Crayston JA, Walton JC, Worsfold DJ. *Tetrahedron Lett* 1990;31:771–4.
- [4] (a) Suguro M, Iwasa S, Kusachi Y, Morioka Y, Nakahara K. *Macromol Rapid Commun* 2007;28:1929–33; (b) Yoshikawa H, Kazama C, Awaga K, Satoh M, Wada J. *Chem Commun* 2007;30:3169–70; (c) Nakahara K, Iriyama J, Iwasa S, Suguro M, Satoh M, Cairns EJ. *J Power Sources* 2007;163:1110–3; (d) Nakahara K, Iriyama J, Iwasa S, Suguro M, Satoh M, Cairns EJ. *J Power Sources* 2007;165:398–402; (e) Nakahara K, Iwasa S, Iriyama J, Morioka Y, Suguro M, Satoh M, et al. *Electrochim Acta* 2006;52:921–7; (f) Satoh M. *NEC J Adv Technol* 2005;2:262–3; (g) Satoh M, Nakahara K, Iriyama J, Iwasa S, Suguro M. E87-C. *Rev Int Criminol Police Tech IEICE Trans Electron* 2004;2076; (h) Nakahara K, Iwasa S, Satoh M, Morioka Y, Iriyama J, Suguro M, et al. *Chem Phys Lett* 2002;359:351–4.
- [5] (a) Nishide H, Oyaizu K. *Science* 2008;319:737–8; (b) Suga T, Konishi H, Nishide H. *Chem Commun* 2007;17:1730–2; (c) Nishide H, Suga T. *Electrochem Soc Interface* 2005;14:32–6; (d) Nishide H, Iwasa S, Pu YJ, Suga T, Nakahara K, Satoh M. *Electrochim Acta* 2004;50:827–31.
- [6] (a) Katsumata T, Qu J, Shiotsuki M, Satoh M, Wada J, Igarashi J, et al. *Macromolecules* 2008;41:1175–83; (b) Qu J, Katsumata T, Satoh M, Wada J, Igarashi J, Mizoguchi K, et al. *Chem Eur J* 2007;13:7965–73; (c) Qu J, Fujii T, Katsumata T, Suzuki Y, Shiotsuki M, Sanda F, et al. *J Polym Sci Part A Polym Chem* 2007;45:5431–45; (d) Katsumata T, Satoh M, Wada J, Shiotsuki M, Sanda F, Masuda T. *Macromol Rapid Commun* 2006;27:1206–11.
- [7] Qu J, Katsumata T, Satoh M, Wada J, Masuda T. *Macromolecules* 2007;40:3136–44.
- [8] Qu J, Khan FZ, Satoh M, Wada J, Hayashi H, Mizoguchi K, et al. *Polymer* 2008;49:1490–6.
- [9] Qu J, Morita R, Satoh M, Wada J, Terakura F, Mizoguchi K, et al. *Chem Eur J* 2008;14:3250–9.
- [10] Allcock HR, Bender JD, Morford RV, Berda EB. *Macromolecules* 2003;36:3563–9.
- [11] Sutthasupa S, Terada K, Sanda F, Masuda T. *J Polym Sci Part A Polym Chem* 2006;44:5337–43.